Chirp-Controlled Tandem Electroabsorption Modulator Integrated with an SOA and a Sampled-Grating DBR laser

Leif A Johansson[1], Yuliya A Akulova[2], Greg A Fish[2] and
Larry A. Coldren[1]

[1]Unversity of California, Santa Barbara, ECE Dept. [2]Agility Communications, Inc.

Abstract: Chirp compensation is demonstrated using voltage division to a long-section electroabsorption phase modulator together with an amplitude modulator arranged in a tandem configuration, both integrated with an SOA and a sampled-grating DBR laser.

Keywords: Time-resolved chirp, Optical modulation, Monolithic integration, Tunable laser.

1. Introduction

The normally positive chirp of electroabsorption modulators is a limiting factor for data transmission over long spans of fiber. For QCSE modulators, this limitation can be addressed by achieving a negative chirp factor using special quantum-well structures [1]. For integration of an EAM with a widely-tunable laser, a Franz-Keldysh modulator is however preferred because of the wider spectral bandwidth compared to QCSE modulators [2]. In this case, an alternative approach is needed in order to achieve negative chirp operation. One method that has been proposed [3] is using two EA modulators in a tandem configuration, one biased for amplitude modulation, the other biased for phase modulation using an inverted driver signal. This approach is limited by the voltage swing available at the phase modulator, determined on the high voltage side by the diode threshold voltage, where carrier injection is causing distortion, and limited on the low voltage side by the onset of absorption that ultimately makes the insertion loss prohibitive and deteriorates the extinction ratio. One possibility to enhance the available performance of this approach is to use different bandgap EA-modulators, possible to achieve using quantum-well intermixing techniques [4]. A second possibility that applies to Franz-Keldysh modulators is to use a simple voltage division scheme, which is described in this paper.

2. Device design

The devices used here are similar to the one described in [2], where more than 10mW output power, lower than 2MHz linewidth, and more than 40dB sidemode suppression ratio is achieved over more than 40nm wavelength tuning range. The difference to those in [2] is that the electroabsorption modulator is split in two parts arranged in a tandem configuration. Figure 1 shows a schematic of the device used in this work. Also shown in fig.1 is a schematic of the voltage division scheme used. The device is mounted onto an Aluminum Nitride RF carrier, with integrated thin-film resistors. The amplitude modulator is terminated in parallel to 50Ω in series with a capacitor. In contrast, the phase modulator is terminated in parallel by a lower value resistor and in series by a second resistor, such that $R_1+R_2=50\Omega$. The resulting voltage division factor, n, is given by $n=50\Omega/R_1$. To compensate for the lower modulation voltage, the phase modulator is made n times longer than the amplitude modulator. To a first order estimate, the RC-limited bandwidth of the modulators remains the same. The main advantage of the described voltage division scheme is that while the modulation voltage is now scaled down by a factor of n, the threshold voltage stays constant, increasing the available phase swing while keeping amplitude modulation in the phase modulator low. Two devices are investigated, the first having a 200μm amplitude modulator and an 800μm phase modulator, with a voltage division factor of $n=4$. The second device has equal length sections of 120μm, and is used for verification of the benefits of the principle.

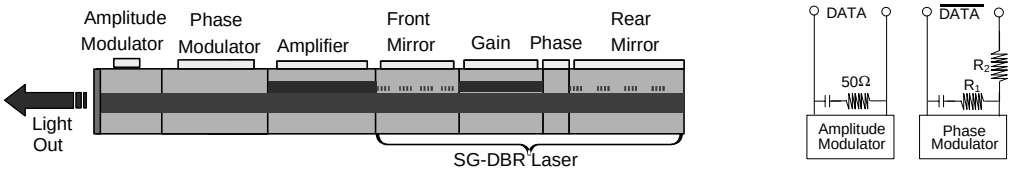

Figure 1: Left shows a schematic of the tandem EAM modulator, integrated with an SOA and a sampled-grating DBR laser. To the right a simple schematic of the voltage division scheme is shown.

3. Experiment

A 2.5Gb/s datastream was used to modulate the amplitude modulator, while the data-bar output of the Agilent 70842B bit error rate tester was used to modulate the phase modulator. The time-resolved chirp characteristics of the modulated optical signal is measured using an Advantest Q7606B optical chirp form test set and an Agilent 86100A oscilloscope. The effective chirp factor, α_{eff}, is then derived from the time-resolved chirp data. Previously, using an amplitude modulator only, the effective chirp parameter has been shown to correlate well to the fiber dispersion penalty for this type of devices [5]. By varying the attenuation/amplification of the signal applied to the phase modulator, the resulting chirp of the device can be controlled. Figure 2 shows the measured chirp forms for the device when voltage division was used. The phase modulator was biased at 0V and the

amplitude modulator at –2.6V. The left plot shows the chirp characteristics of the amplitude modulator alone, corresponding to an α_{eff} of 0.97. Applying a modulation signal to the phase modulator of equal amplitude as to the amplitude modulator, results in the characteristics shown by the center plot, corresponding to α_{eff} of 0.03. The remaining frequency chirping, particularly apparent at the falling edge, is a result of different impulse response between the phase and amplitude modulator. The different impulse response can be attributed in part to the inductance of the bondwire used to connect the modulators to the RF lines of the carrier. A more careful RF design should further decrease the envelope of the frequency chirp. The plot at the right shows α_{eff} of -0.86 for a phase modulation signal amplified by 3dB relative to that of the amplitude modulator.

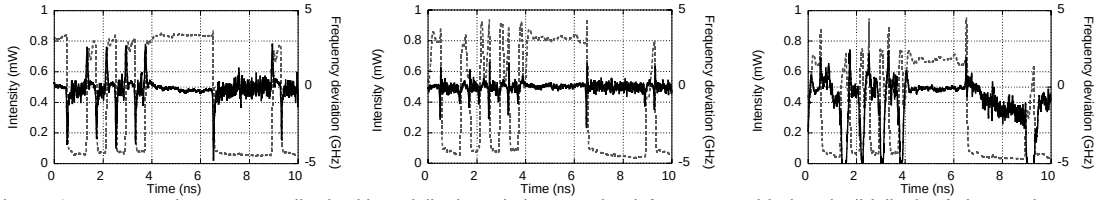

Figure 2 : Measured output amplitude (dotted line) and time-resolved frequency chirping (solid line) of the tandem EAM conficuration. The resulting effective chirp factors are 0.97, 0.03 and -0.86, respectively from left to right.

Figure 3 shows a comparison between the performance of a device using voltage division and a control device with equal length modulators. The left plot shows the resulting effective chirp factor. It is seen that the control device achieves negative chirp with lower phase modulation voltage. The cause for this is believed to be localized heating at the front edge of the phase modulator that for the control device experiences significant optical absorption, with the higher applied modulation voltage and therefore necessarily lower bias point: -2V. The benefits of the voltage division scheme is clearly observed in the plot to the right, where the extinction and excess insertion loss compared to amplitude modulation only, is shown. Significant penalties are shown for the control device at lower chirp values, as a result of counteracting amplitude modulation in the phase modulator. Using voltage division, α_{eff} down to -0.3 is observed with <2dB excess insertion loss and <1dB degradation of extinction ratio. For lower values of chirp, further degradation is observed, partly due to too high applied voltage to the phase modulator, evident in the more distorted chirp form shown in Fig. 2, right. This can be traded off with a slightly degraded insertion loss and extinction by lowering the bias point of the phase modulator.

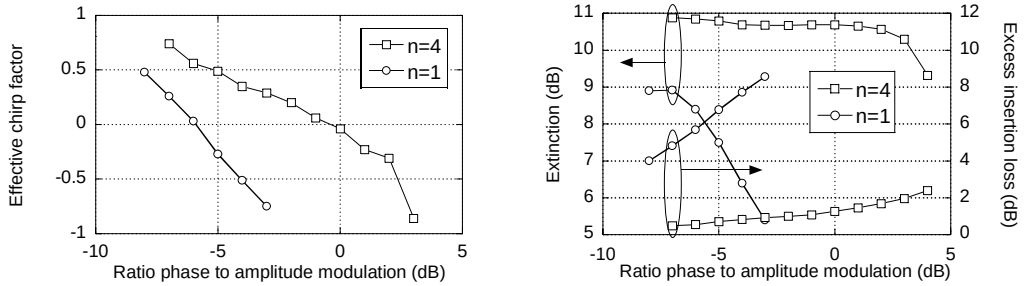

Figure 3: Left plot shows measured large-signal chirp factor for n=4 and n=1, as a function of the ratio of phase-modulator drive signal to amplitude-modulator drive signal. Right plot shows the corresponding extinction ratio and resulting penalty in terms of insertion loss, compared to amplitude modulation only.

4. Conclusion

We have demonstrated how two Franz-Keldysh modulators arranged in a tandem configuration can used to produce chirp-controlled optical modulation with an effective chirp factor down to -0.86. It is shown how using a long phase modulating section in combination with simple voltage division scheme to one of the modulator sections can improve the performance of the tandem modulator to <2dB excess insertion loss and <1dB degradation of extinction ratio compared to a single section modulator for effective chirp factors down to -0.3.

References

[1] M. Kato and Y. Nakano, "Strain-compensated InGaAs/InAlAs/InP pre-biased quantum well for polarization-insensitive and negative-chirp electro-absorption optical modulators, " *Indium Phosphide and Related Materials 2000*, pp. 404-407, May 2000.

[2] Y. A. Akulova, G. A. Fish, P. C. Koh, C. Schow, P. Kozodoy, A. Dahl, S. Nakagawa, M. Larson, M. Mack, T. Strand, C. Coldren, E. Hegblom, S. Penniman, T. Wipiejewski, and L. A. Coldren, "Widely-Tunable Electroabsorption-Modulated Sampled Grating DBR Laser Transmitter", *IEEE J. Selec. Top. in Quantum Electron.*, 8, 1349-1357, Nov/Dec 2002.

[3] M. Claassen, W. Harth and B. Stegmüller, "Two-section electroabsorption modulator with negative chirp at low insertion loss," *Electron Lett.,* **32**, 2121-2122, 1996.

[4] E.J. Skogen, J.S. Barton, S.P. Denbaars and L.A. Coldren, "A quantum-well-intermixing process for wavelength-agile photonic integrated circuits*," IEEE Seected. Topics in Quantum Electronics*, **8**, pp. 863-869, Jul/Aug, 2002.

[5] P.C. Koh, C. Schow, Y.A. Akulova and G.A. Fish, "Correlation between dispersion penalty and time-resolved chirp for widely tunable electroabsorption-modulated SGDBR laser across the EDFA gain bandwidth," *IEEE Photon. Technol. Lett.,* **15**, 1011-1013, July 2003.